JOURNAL OF Applied Polymer SCIENCE

Synthesis and Thermal Properties of Bismaleimides with Mesogen Aromatic Amide–Ester and Flexible Polymethylenic Group

Bernard Fache,[1] Bernard Gallot,[2] Marie Pierre Gelin,[1] Jean Claude Milano,[1]* Quang Trung Pham[1]

[1]Laboratoire des Matériaux-Polymères-Interfaces-Environnement Marin (MAPIEM EA 4323), Université du Sud Toulon Var, La Garde, France

[2]Laboratoire des Matériaux Organiques à Propriétés Spécifiques—C.N.R.S., 69390 Vernaison, France

*Correspondence to: J. C. Milano (E-mail: jcmilano@univ-tln.fr)

ABSTRACT: Four bismaleimides with mesogen "amide–ester" aromatic and flexible polymethylenic group variable length ($8 \leq n \leq 11$) were synthesized in two stages, producing yields exceeding 80%. These bismaleimides (BMIs) were obtained after several purifications by dissolution—precipitation in dimethylformamide–methanol (1/4) with over 94% purity (high-performance liquid chromatography). These pure BMIs were characterized by nuclear magnetic resonance, Fourier transform infrared spectroscopy, and elemental analysis and studied by differential scanning calorimetry, thermogravimetric analysis, polarized light microscopy, and X-ray diffraction. Solubilities and thermal properties show effects of parity. The even BMIs are more difficult to solubilize than the odd BMI. The melting points of the even BMI (approximately, 220°C) are far higher than those of odd BMI (approximately, 160°C). Crosslinking temperatures of even BMI are close to 230°C, whereas odd BMI crosslinking temperatures are higher (approximately, 250°C). Even BMIs give rise to a liquid crystal state upon melting. Under the same conditions, odd BMIs give rise to an amorphous state; however, after crosslinking, the four bismaleimides give rise to an ordered liquid crystal state of smectic type. © 2012 Wiley Periodicals, Inc. J. Appl. Polym. Sci. 000: 000–000, 2012

KEYWORDS: polyimides; liquid crystal; synthesis; thermal properties; structure–property relations

Received 24 May 2011; accepted 8 March 2012; published online 00 Month 2012
DOI: 10.1002/app.37659

INTRODUCTION

The bismaleimides enable the production of adhesives and high-performance composite materials. They are thermostable and are used more and more to replace polyepoxides. The bismaleimides are mainly used in aeronautic, space, electronic, and military equipment. However, they show some defects. They are easy to use (thermal crosslinking), but they typically have high melting points and the rate of crosslinking is too fast. Hence, little is known about solubilities and they are hardly soluble in common solvents. Additionally, the resulting materials are often brittle owing to a very high density of crosslinking. Therefore, to solve these problems, much research work has been carried out. Indeed, the bismaleimides have a very interesting development potential. This research is important in scientific and technological fields. For example, much work is being carried out to improve their mechanical properties.

Two areas of research have developed in this field. The first line of research is lengthening of bismaleimide (BMI) molecules: Long and flexible BMI molecules are effective in reducing crosslinking density. Elongation of the BMI is carried out by incorporating groups which can be aromatic,[1–3] heterocyclic,[2,4–6] ester,[4,7–9] ether,[4,8,10,11] amide,[11,12] or flexible spacers of variable lengths[7,13–20] between the maleimides. These BMI can contain silicon,[1,16,17] phosphorus,[21] sulfur,[7,18] and halogens.[7,22] These diverse architectures enable the establishment of correlation structure properties.[1–29] Another line of research is to formulate the most interesting BMI with chemically inert[26] compounds (thermoplastics, elastomers) or, chemically reactive compounds such as diamines[7,28–30] (polyaspartimides), epoxides,[31,32] cyanates,[33–37] allylic (and allylphenolics),[38–41] olefins,[42,43] propargyls ethers,[44] and nanoparticles (nanocomposites). This chemistry is rich, interesting and there are many scientific publications.[45–61]

In recent years, another concept has been studied: bismaleimides liquid crystals (BMI LC). They belong to a new family of polymeric materials—thermoset liquid crystals (CLT).[62,63] The "conventional" BMI produce, after crosslinking, amorphous materials. Like CLT, the BMI LC crosslink in an ordered liquid crystal state. The initial work on the CLT concerned diacrylate

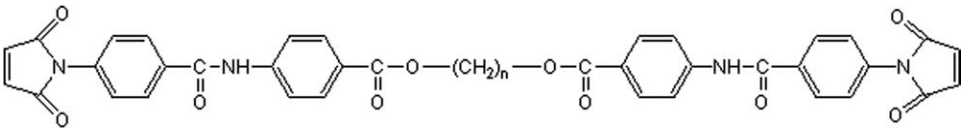

Figure 1. Structures of the synthesized BMI. $n = 8, 9, 10, 11$.

liquid crystals[64,65] and diepoxide liquid crystals.[66–75] Work on diepoxides LC, which are currently the most numerous,[76–81] showed that the liquid crystal nature of crosslinked material could improve the mechanical and thermal properties of polyepoxides. The first BMI LC were synthesized and characterized in the USA in 1990 by Hoyt and Benicewicz.[82,83] These BMIs of "arylate" or "aramide" structure allow the production of crosslinked polybismaleimides of nematic type. In 1995, Hoyt and Huang[84] prepared eutectic mixtures between two of the BMIs published in 1990. This method makes it possible to decrease the melting points. Since then, other BMI LC have been synthesized.[14,85–92] They have a great diversity of molecular structures, and reveal on heating either nematic mesophases[85–92] or smectic mesophases.[14]

During the course of our research, four BMI LCs were synthesized (Figure 1). They were purified, analyzed by high-performance liquid chromatography (HPLC), and characterized by nuclear magnetic resonance (NMR) and Fourier transform infrared spectroscopy (FTIR). After purification, the thermal properties of these BMIs were studied by differential scanning calorimetry (DSC), thermogravimetric analysis (TGA), hot-stage polarized light microscopy (PLM), and X-ray diffraction (X-R). This study allowed structure–property relationships to be established and contributed to the explanation of these correlations.

EXPERIMENTAL

Materials and Analyses

All the reagents and the solvents, used without further purification, were purchased from Aldrich.

Purification of BMI. After synthesis, the BMI solid was then dissolved in dimethylformamide (DMF) (1 volume) and precipitated in methanol (4 volumes). The operation is carried out several times.

Analyses After Purification. The ^{1}H-NMR spectra were recorded on a BRUKER spectrometer (400 MHz) with deutered dimethyl sulfoxide (DMSO) as solvent. All spectra were obtained with tetramethylsilane (TMS) as an internal standard. The FTIR spectra were recorded on an Infrared Fourier Transform spectrophotometer NICOLET. The IR spectra were obtained with KBr pellets. Calorimetric studies were carried out with a DSC TA Instrument thermal analyzer DSC Q10 and DSC Q100 with a scan rate of 10 and 20°C/min. Thermogravimetric analyses (TGAs) were performed under inert and air atmosphere at a heating rate 10°C/min up to 800°C with a TGA Q100 TA Instrument thermogravimetric analyzer. The degradation temperatures (Td_1 and Td_2) are determined at the inflexion points of the TGA curves. Transition temperatures and textures were observed in Polarized Light with an OLYMPUS Microscope equipped with a METTLER FP 90 plate heating system (PLM). X-R experiments were performed on unoriented samples with a home-made pinhole camera, operating under vacuum, using Ni-filtered Cu radiation ($\lambda = 1.54$ Å) provided with a SIEMENS tube operating at 36 KV and 30 mA. This camera was equipped with an electric heating device operating between 20 and 300°C with an accuracy of 1°C. The synthesized BMIs were analyzed by chromatography in liquid-phase high performance (HPLC-GILSON) in isocratic conditions starting from a C18 column (reversed phase) and UV detection at 254 nm. The derivative "monomaleimide" was synthesized in the laboratory by reacting diamine D11 (1 mmol) with the *p*-maleimidobenzoyl chloride (1 mmol). The mixture obtained was directly used as standard HPLC. Solubilities were worked out by experiments using concentrations of 10 mg of product in 1 mL of solvent. The solubility is measured after 10 min of contact. The compounds tested were classified as soluble (++), insoluble (−), soluble when heated (+), or partially soluble when heated (±); the solution was maintained at 60°C for 5 min.

Results of the elementary analysis of these BMIs carried out on the four elements (C, H, O, and N) are correct. The differences between theoretical and experimental values were always lower than 3.6%.

BMI $n = 8$					
($C_{44}H_{38}O_{10}N_4$) (782)					
Calc	C 67.52	H 4.86	N 7.16	O	20.46
Found	C 67.65	H 4.92	N 7.15	O	21.19
BMI $n = 9$					
($C_{45}H_{40}O_{10}N_4$) (796)					
Calc	C 67.84	H 5.02	N 7.04	O	20.10
Found	C 67.02	H 5.17	N 6.95	O	20.36
BMI $n = 10$					
($C_{46}H_{42}O_{10}N_4$) (810)					
Calc	C 68.15	H 5.19	N 6.91	O	19.75
Found	C 67.31	H 5.30	N 6.87	O	20.15
BMI $n = 11$					
($C_{47}H_{44}O_{10}N_4$) (824)					
Calc	C 68.45	H 5.34	N 6.79	O	19.42
Found	C 67.66	H 5.53	N 6.90	O	19.58

Syntheses

Synthesis of the 4-Maleimidobenzoic acid. In total, 460 mmol of 4-aminobenzoic acid is dissolved in 400 mL of anhydrous DMF. Then, 460 mmol of maleic anhydride is added slowly at room temperature. The mixture is agitated at room temperature for 1 h. The acetic anhydride (650 mmol) and the sodium

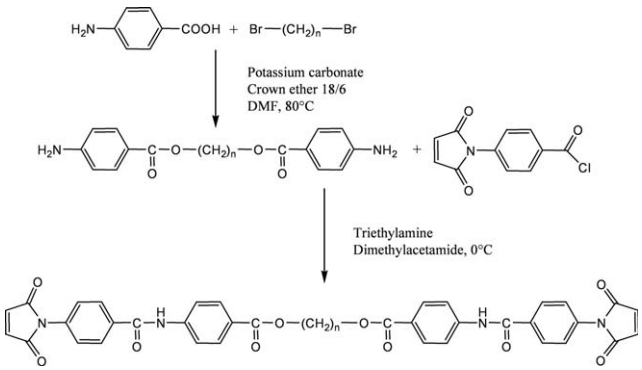

Figure 2. Synthesis of BMI "aramide–arylate" with flexible polymethylenic group.

acetate (46 mmol) are then added and the mixture is heated to 45°C for 2 h. After the reaction, the mixture is poured into 2 L of water. The precipitate obtained is filtered and washed with water. The product is dried under vacuum. It appears as a white powder. ^{1}H-NMR (DMSO): δ° 8.06 (2H,d), 7.51 (2H,d), 7.23 (2H,s), 13.07 (1H,s). ^{13}C-NMR (DMSO): C 169.1; 166.3; 135.1; 134.5; 129.5; 129.2; 125.7.

Synthesis of 4-Maleimidobenzoyle chloride. A mixture of 67.6 g of 4-maleimidobenzoic acid, 400 mL of anhydrous toluene, and 100 g of oxalyl chloride is heated until reflux (approximately, 60°C) for 2 h. At the end of the reaction, the oxalyl chloride excess is removed by flash distillation at room temperature. After filtration and washing with pentane, a brown solid was obtained. It was dried under vacuum for a night before being used for the following stage. ^{1}H-NMR (DMSO): δ° 8.04 (2H,d), 7.50 (2H,d), 7.21 (2H,s).

Synthesis of Diamines α,ω-Bis(4-aminobenzoyloxy) Alkane (D8, D9, D10, and D11). The following mixture is prepared: 500 mL of DMF, 120 mmol of 4-aminobenzoic acid, 300 mmol of potassium carbonate, 5 mmol of crown ether, and 50 mmol of α,ω-dibromoalcane. This mixture is agitated at 80°C for approximately 5 h. Then, it is cooled to room temperature and is poured into ice water. A precipitate is formed. After filtration, the white solid obtained is washed with 8% sodium hydroxide solution. After an hour's agitation, the powder is again recovered by filtration (filtrate pH > 7). This powder is washed in 800 mL of water and filtered. After several washings, carried out

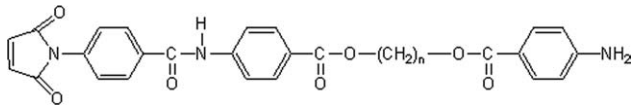

Figure 3. Structure of "monomaleimide."

until the pH of the water is neutral, the powder is recovered, spread out, and dried under vacuum. ^{1}H-NMR (DMSO): D8: δ° 7.64 (4H,d), 6.57 (4H,d), 5.99 (4H,s), 4.15 (4H,t), 1.65 (4H,m), 1.34 (8H,m). ^{13}C-NMR (DMSO): D8: C° 165.6; 163.2; 130.7; 115.8; 112.4; 63.2; 28.4; 28.1; 25.2.

Synthesis of the BMI (B8, B9, B10, and B11). A solution of 25 mmol of diamine in 200 mL of anhydrous dimethylacetamide (DMAc) is kept at a temperature of approximately 0°C. Then, 50 mmol of triethylamine is added. Finally, the 4-maleimidobenzoyl chloride (50 mmol) is added by fractions. The reaction is kept at a temperature close to 0°C for 2 h. The solution browns. After cooling to room temperature, the mixture is filtered and then precipitated in 800 mL of water. The solid obtained is washed with 900 mL of acidified water and again washed several times with pure water.

RESULTS AND DISCUSSION

Syntheses

The synthesis of these BMIs was conducted in two main steps. The first step provided a symmetric "diamine" having polymethylene flexible grouping of variable length. The flexible group is located in the center of the molecule (Figure 2). This compound was obtained from dihalides (Figure 2). These diamines (D8, D9, D10, and D11) were synthesized in the presence of potassium carbonate giving very good yields (>80%) using DMF solvent and crown ether as phase transfer catalyst.[74] Then, the BMIs (B8, B9, B10, and B11) were prepared by the reaction of *p*-maleimidobenzoyl chloride on the amino groups. The three-step synthesis of *p*-maleimidobenzoyl chloride is well documented.[93] Using this method, the BMIs were obtained in good conditions with very high yields (Table I). The first purification in aqueous acid (**Experimental** section) allows products with purity ranging from 72 to 94%, according to synthesis, to be obtained (Table I).

This level of purity may be sufficient for the main applications of the BMI in the field of composite materials or adhesives. Indeed, according to the reaction mechanisms, two groups of

Table I. Yields for the Syntheses (BMI LC and Intermediaries)[a]

	Yields for the syntheses (%)			Rate of purity of the BMI LC (%)		
					After purification	
n	AMB	Diamine	BMI	After synthesis	Before corrections	After corrections
8	93	89	90	94[b]	98	95
9	93	80	89	72[b]	97	96
10	93	92	75	87[b]	96	94
11	93	85	92	75[b]	97	96

[a]Yields of the BMI LC were obtained after the purification with the acid envisaged in the protocol of synthesis (before the purifications by precipitations). Purities of BMI LC obtained by HPLC at 254 nm, [b]The purities provided after synthesis are not corrected.

Table II. B11 Purification—Melting Points (T_f: Peak of the Endotherm DSC) and Results of ^{1}H-NMR Analysis[a]

Precipitation	T_f (°C)	^{1}H-NMR
After synthesis	150.6	Impurities observed[b]
1	158.9	Impurities observed[b]
2	158.4	Impurities not observed
3	160.1	Impurities not observed
4	163.5	Impurities not observed
5	165.7	Impurities not observed
6	164.2	Impurities not observed

[a]The impurities correspond to the signals of the AMB, diamine D11, and the monosubstituted compound, [b]Spectra, Figure 7.

impurities are *a priori* possible. The reagents which were used in the last step are the first group of impurities. In general, the double substitution reactions are not quantitative. Also, diamine, *p*-maleimidobenzoic acid and *p*-maleimidobenzoyl chloride residues are present at the end of synthesis. Indeed, in the presence of water, unstable *p*-maleimidobenzoyl chloride easily converts to the *p*-maleimidobenzoic acid. The second group of impurities which could be present: byproducts created from these double substitution reactions. The formation of a monosubstituted derivative "monomaleimide" (Figure 3) was predictable. Finally, according to Loustalot et al.[58] and Curliss et al.,[50] during these reactions, the formation of a product of ring opening by aminolysis was also possible. At the end of the synthesis, four of these five possible impurities were identified by NMR and HPLC. The product that could have formed by ring opening was not detected. However, these four highly reactive compounds (diamine, *p*-maleimidobenzoic acid, *p*-maleimidobenzoyl chloride, and monomaleimide) can react thermally with the synthesized BMI. Indeed, when the BMI is used as adhesive or thermosetting resin, during the heating phase, these impurities will be able to react on the BMI synthesized by copolymerization or the Michaël reaction. These impurities will be involved in the production of the final three-dimensional networks. When crosslinking is well conducted, nothing remains of the free impurities in this network. Moreover, with "conventional" BMI in the field of applications incomplete synthesis processes are sometimes sought-after. With the COMPIMIDE concept, for example, the BMI and its monomaleimide are crosslinked in the mold by heating only.[94]

But characterization of mesomorphic properties with these BMIs requires a high degree of purity. The search for correlation structures–properties also requires maximum purity. However, levels of purity of BMI obtained after synthesis are not adequate. Also, these BMIs were purified by dissolution and precipitation.

Purification

Purification of the BMI was conducted using selective solvents. This simple method made it possible to purify the poorly soluble compounds in volatile solvents frequently used for recrystallization or column chromatography. These highly polar BMIs were purified in two steps. First, the mixture obtained after

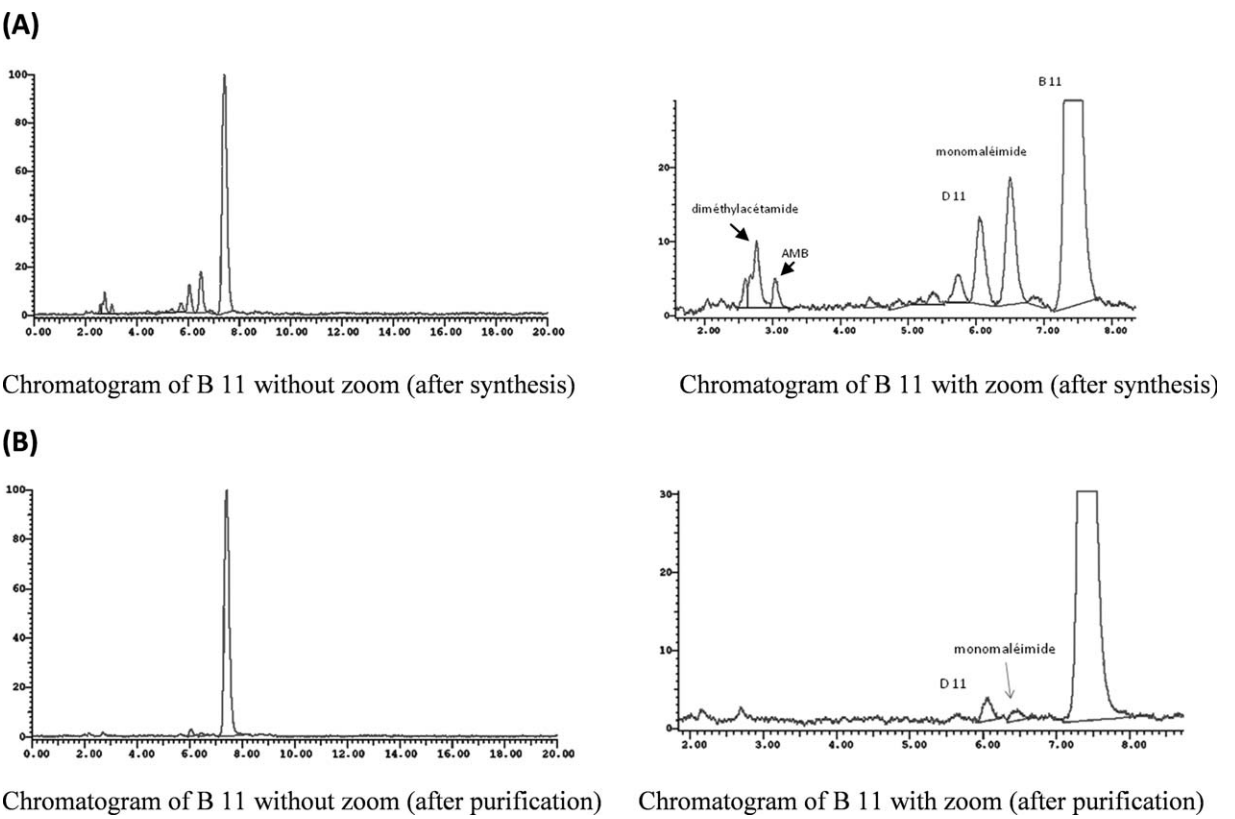

Figure 4. HPLC chromatograms of B11 (example) before (A) and after (B) phases of purification by dissolution–precipitation.

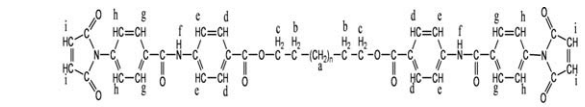

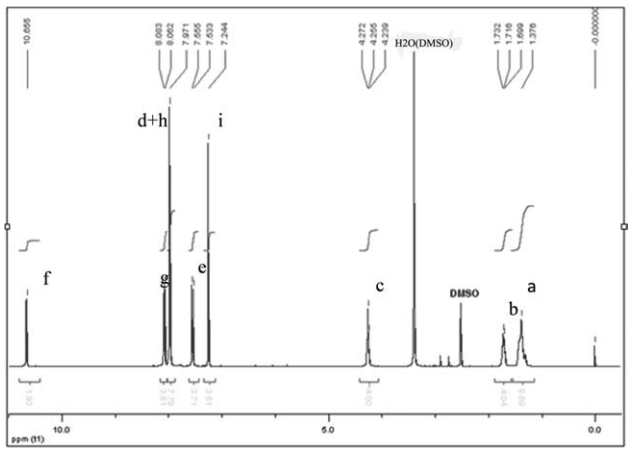

Figure 5. [1]H NMR of B8.

synthesis is dissolved in DMF (1 volume). Then, the BMI is precipitated by addition of methanol (4 volumes). After several dissolution/precipitations, high-purity BMI is obtained. The purification is considered valid when the melting point of the BMI remains constant between the two dissolution/precipitations. B11 purification is provided as an example in Table II. For each dissolution/precipitation, a thermogram DSC and [1]H-NMR spectrum were recorded. The products recovered at the second dissolution/precipitation do not show any detectable impurities in [1]H-NMR. However, the DSC study shows a stabilization of the melting point at the end of the fifth dissolution/precipitation (Table II). B11 (taken as an example) was regarded as pure starting from the fifth dissolution/precipitation. The properties of the four BMIs were studied after five to six dissolution/precipitations.

HPLC Analysis

Purified BMI B8, B9, B10, and B11 were analyzed by HPLC, but these BMIs are poorly soluble in solvents usually used in HPLC. Also, an eluent has been specifically developed to work in an isocratic system. The eluent contains 3% of DMF and 97% of the mixture EB (EB consists of 13% of THF and 87% of the mixture of acetonitrile–water 80 : 20). THF and DMF are not often used in isocratic reverse-phase HPLC. However, they have viscosities which are not too high and excellent UV purities. They enabled the obtention of a good eluent effective for all of the BMI. A small amount of orthophosphoric acid was added to the mixture of acetonitrile–water 80 : 20 (0.1% in acetonitrile). This change in pH makes it possible to decrease the retention time of polar compounds, particularly basic compounds such as diamines. It also limits losses of the polar compounds in the column. It has been shown that BMIs obtained after synthesis (before purification by dissolution and precipitation) exhibit rates of purity HPLC ranging from 72 to 94% (Table I). These levels of purity were identified at 254 nm without correction. In reality, they are slightly lower. The corrected values take into account the response factors of the BMI and the impurities at 254 nm[15] (Table I). The qualitative HPLC analysis was conducted on the basis of the reference compounds (standards). The following impurities were detected, in order of retention times, dimethylacetamide (solvent of BMI synthesis), *p*-maleimidobenzoic acid (impurity produced by hydrolysis of *p*-maleimidobenzoyl chloride), *p*-maleimidobenzoyl chloride (unstable in the presence of water: not systematically observed), diamine, and "monomaleimide" (monosubstituted diamine). Monomaleimide appears in our HPLC conditions between D11 and B11 (Figure 4). The purity levels are summarized in Table I. After purification by dissolution/precipitation, using DMF–methanol (1/4), purity levels are between 94 and 96%. The BMI chromatograms obtained after purification show only residual presence of traces of diamine or diamine and monomaleimide (B11 example: Figure 4).

Characterization of BMI with [1]H-NMR, [13]C-NMR, and FTIR

[1]H-NMR of these BMIs obtained after purification show three types of signals (the [1]H-NMR spectrum of B8 interpreted is given as an example in Figure 5): signals located between 0 ppm (TMS) and 5 ppm; signals present between 6 and 9 ppm and the signal appearing beyond 10 ppm. The signals ranging from 0 to 5 ppm belong to the methylenic protons of the flexible group (—CH_2—). The second group of signals present in [1]H-NMR spectra, located between 6 and 9 ppm, corresponds to the protons carried by the carbon atoms sp.[2] The most shielded singlet, at approximately 7.1 ppm, corresponds to ethylene protons of maleimide. The other signals, comprising two doublets and a singlet located between 7.4 and 8.1 ppm, correspond to resonance of the protons of the aromatic groups. Finally, the signal (singlet) located beyond 10 ppm is owing to the protons of the amide groups. [13]C-NMR spectra can also be divided into three parts (the interpreted spectrum of B8 is provided as an example in Figure 6). The area between 180 and 160 ppm corresponds to the resonance of carbon atoms of carbonyl groups. The signals of carbons of ethylene and carbons of aromatic are located between 150 and 110 ppm. Finally, between 80 and 10 ppm are the signals of aliphatic carbon atoms forming flexible groupings. The NMR spectra (proton and carbon) of the BMI

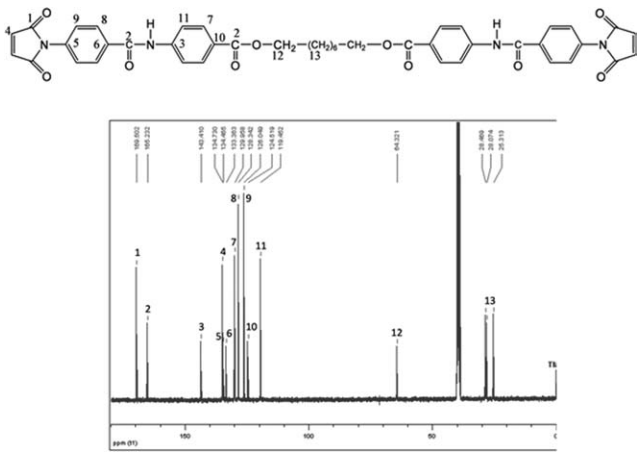

Figure 6. [13]C NMR of B8.

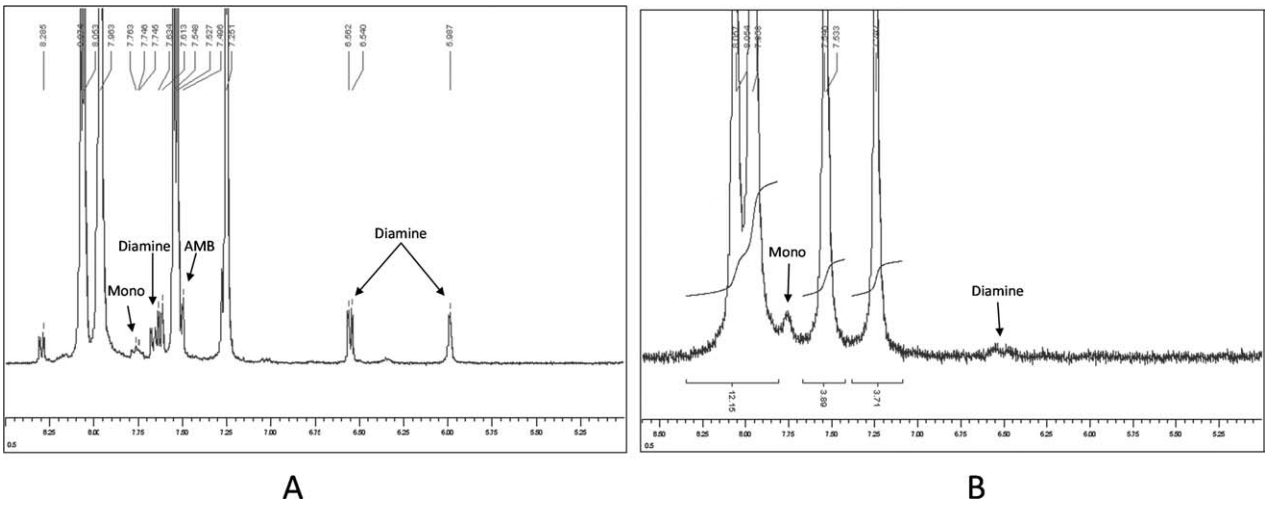

Figure 7. ^{1}H NMR spectra of B11 (example) obtained after synthesis (A) and four precipitations (B) (DMF/methanol).

after purification show an absence of impurities[15] (Figures 5 and 6, and **Experimental** section). The ^{1}H-NMR spectra of the BMI obtained after purification (example B8: Figure 5) do not show 4-maleimidobenzoic acid (AMB) or 4-maleimidobenzoyle chloride (CMB) signals. They show no signals characteristic of diamines.[15] When diamines are present as impurities in BMI, the signals from 7.6, 6.5, 5.9, and 4.1 ppm are clearly visible (Figure 7). The protons at 7.6, 6.5, and 5.9 ppm are characteristics of these aromatic diamines. The signal at approximately 4.1 ppm corresponds to aliphatic protons on carbons located in α of esters groups. They are shielded compared to their BMI homologs.[15] Indeed, compared to the same protons of the BMI, the protons located in α ester group are shielded by the presence of amine groups bonded to aromatic rings. These diamine groupings are, in this configuration, electron donors by mesomeric effect. For every BMI obtained after purification, the absence of ^{13}C-NMR signals characteristic of diamines and AMB was observed[15] (4.15 ppm for D8 [**Experimental** section] and 4.27 ppm B8 [Figure 5]). In addition to the potential characterization of impurities owing to reagents used (**Experimental** section and Figure 6), ^{13}C-NMR makes it possible to characterize a possible chemical evolution of the BMI. Indeed, these BMIs can react during their synthesis or during different stages of purification. For example, during the BMI purification, solvents are removed by heating. If these steps of heating are not conducted carefully, they can cause polymerization of BMI to start (homopolymerization). These stages of heating can also create side reactions between the BMI and their impurities (Michaël). On ^{13}C-NMR spectra of purified BMI, there are no signals at approximately 176, 175, 174, 51, 42, and 36 ppm. However, signals at 175 and 42 ppm are owing to BMI homopolymerization.[58] Other signals at 176, 174, 51, and 36 ppm correspond to signals created by the addition of Michaël between a BMI and a diamine.[58] After purification of the BMI, these signals were not detected.

Infrared spectra (FTIR) of pure BMI are identical. FTIR of B11 spectrum is provided as an example (Figure 8). The main absorption bands (in cm^{-1}) of these BMIs are summarized in Table III. A comparison of D11 and AMB spectra with B11 spectrum (Figure 8) confirms the absence of these impurities.[15] The most important and specific bands of the diamine (3400, 3347.83, and 3239.13 cm^{-1}) and *p*-maleimidobenzoic acid (broadband, 3147.83 cm^{-1}) are absent on B11 IR spectrum.[15] Homopolymerization can also be characterized by FTIR[56] but the characteristic band of this evolution was not observed (succinimide group: γ [C—N—C] between 1185 and 1190 cm^{-1}).

Solubility

The results of tests of solubility carried out on four BMIs and their main impurities (AMB and diamines) are summarized in Table IV. Two general comments can be made. First, the four BMIs are poorly soluble. B9 is the most soluble, whereas the B8 is the least soluble. Indeed, B9 is cold soluble in 14 solvents (38 tested solvents). B8 is soluble in eight solvents. In contrast, the AMB and D9 (examples of impurities) are, respectively, cold soluble in 22 and 17 solvents (Table IV). Second, even BMIs are more difficult to dissolve than odd BMI, B8 and B10 are cold soluble in eight solvents, whereas odd BMI B9 and B11 are, respectively, cold soluble in 14 and 13 solvents. When heated, odd BMIs are partially soluble in butyrolactone, diacetone alcohol, triallylcyanurate, and DMF–toluene mixture (1/20), whereas

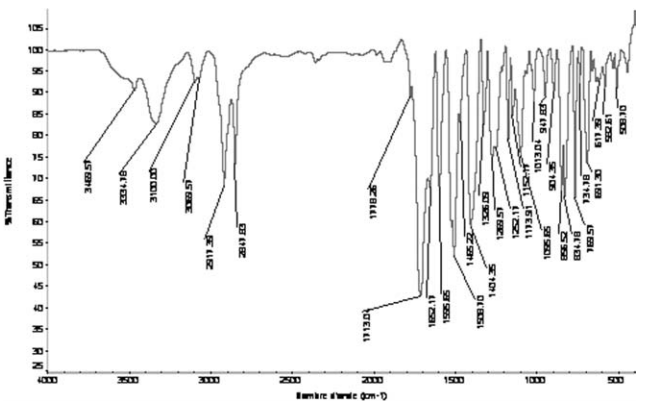

Figure 8. FTIR spectrum of B11 pure.

Table III. Principal Signals FTIR of B11 (in cm^{-1})

Absorption band	Identification
3469.57	Stretching (—N—H—) free of the **amide** groups
3334.78	Stretching (—N—H—) related **amides** groupings
3100	Stretching (=CH—) **maleimide** groups
3069.57	Stretching (=CH—) **aromatic** groups
2917.39	Asymmetric stretching (—CH_2—) **alkane** groups (flexible grouping)
2847.83	Symmetric stretching (—CH_2—) **alkane** groups (flexible grouping)
1778.26	Stretching symmetric or asymmetric of carbonyl of **maleimide** group (—CO—)
1713.04 Large signal	Vibration of symmetrical or asymmetrical of the carbonyl of the **maleimide** group (—CO—); stretching of the carbonyl group **ester** (—CO—)
1652.17	Stretching of the carbonyl of **amide** group (—CO—)
1595.65	Stretching of **Aromatic** groups (C=C)
1508.70	Stretching of **Aromatic** groups (C=C)
1404.35	Stretching of **Aromatic** groups (C=C)
1269.57	Stretching of the **ester** groups (C—O—)
1252.17	Bending vibration δ (CH) of **aromatic** cycles
1173.91	Stretching vibration (—C—N) of the **maleimide** group
1152.17	Stretching vibration (—C—N—C) of the **maleimide** group
1095.65	Bending vibration δ (CH) of the **aromatic** cycles
1013.04	Bending vibration δ (CH) of the **aromatic** cycles
947.83	Stretching or bending vibration of the **maleimide g**roup (—CH=CH—)
904.35	Bending vibration δ (CH) of the **maleimide groups**
856.52	Bending vibration δ (CH *cis*) of the **maleimide groups**
834.78	Bending vibration δ (C=C) of **maleimide groups**
769.57	Bending vibration δ (C—N) of the **maleimide groups**
691.30	Bending vibration δ (C=C—H *cis*) of the **maleimide groups**

under the same conditions even BMIs are insoluble. Even BMIs are also insoluble in TTT + NDAPMA (2/1). Odd BMIs are heat soluble in TTT + NDAPMA (2/1).

Each compound tested (solvents, BMIs, and impurities: AMB and diamines) was characterized by the solubility parameters of Hansen[95–98]: δ, δ_d, δ_p, and δ_h. Solubility parameters δ_d, δ_p, and δ_h relate, respectively, to forces of London, Keesom, and Lewis (hydrogen bonds). The forces of Debye (interactions permanent dipoles/induced dipoles) were neglected by Hansen. From these solubility parameters, "volumes of solubility"[95–98] can be defined ($\delta = [\delta_d^2 + \delta_p^2 + \delta_h^2]^{1/2}$), but by only taking into account the solubility parameters δ_v and δ_h (by taking $\delta_v = [\delta_d^2 + \delta_p^2]^{1/2}$) the representation can be simplified. Indeed, according to the δ_v and δ_h and of the criteria of cold solubility (soluble or insoluble) some "circles of solubility"[99] can be described. In the course of our study, the solubility parameters δ_d, δ_p, and δ_h were provided directly by Hansen[95–98] or were obtained indirectly from semi-empirical calculations.[99–101]

From the results of tests of solubility (Table IV), areas of solubility of the four BMIs have been described. These four BMIs show very similar solubility areas. In the experiment, it is very difficult to distinguish them, and hence only the graph B11 has been traced (Figure 9). In this study, it was used as reference BMI. For each solvent, δ_h and δ_v were calculated[15] from the results provided directly by Hansen.[95–98] When the values were not directly accessible, solubility parameters were calculated[15] from Van Krevelen[99] semi-empirical method. In Figure 9 (B11), only two points are not correct: the one concerning the TTT + NDAPMA mixture (2/1) and the point DMF + chloroform (1/20) mixture. Indeed, the first point is within the "circle of solubility" while B11 is cold insoluble in this mixture. The second point is outside the circle of solubility while B11 is soluble in this mixture. However, it should be noted that TTT + NDAPMA (2/1) mixture solubility parameters are all calculated empirically (to theoretical approximations are added a few empirical approximations). It should also be noted that in this mixture B11 becomes soluble on heating. With DMF + chloroform (1/20) mixture, the parameter calculations are much more reliable. One should note, however, in this mixture only the odd BMIs (B11 and B9) are soluble. Apart from these two points, the results are consistent.

The co-ordinates of the center of the circle obtained graphically indicate the δ_h and δ_v of BMI. Values found for B11 are as follows:

$$\delta_h = 9.8\,J^{1/2}cm^{3/2}$$

Table IV. Solubilities: BMI, AMB, D8, D9, and D11[a]

No.	Solvent	AMB	B8	B9	B10	B11	D8	D9	D11
1	DMF	++	++	++	++	++	++	++	++
2	DMSO	++	++	++	++	++	++	++	++
3	DMAc	++	++	++	++	++	++	++	++
4	THF	++	±	++	–	++	++	++	++
5	NMP	++	++	++	++	++	++	++	++
6	Py	++	++	++	++	++	++	++	++
7	Acetonitrile	++	–	–	–	–	+	+	+
8	Methanol	+	–	–	–	–	±	+	+
9	Diethylether	–	–	–	–	–	–	–	–
10	Chloroforme	–	–	–	–	–	–	+	+
11	Acetone	++	±	++	–	++	++	++	++
12	Dichloromethane	–	–	–	–	–	–	+	+
13	Ethanol	+	–	–	–	–	–	+	+
14	Toluene	–	–	–	–	–	–	–	–
15	Ethyl-Acetate	+	–	–	–	–	+	+	+
16	Petroleum-Ether	–	–	–	–	–	–	–	–
17	Nitromethane	–	–	–	–	–	–	–	–
18	Acrylonitrile	+	–	–	–	–	±	+	+
19	Butyrolactone	+	–	±	–	±	+	+	+
20	2-Pyrrolidinone	++	+	+	+	+	++	++	++
21	Diacetone alcool	+	–	±	–	±	+	+	+
22	*N,N*-Dimethylacrylamide	++	++	++	++	++	++	++	++
23	1-Vinyl-2-pyrrolidione	++	++	++	++	++	++	++	++
24	Triallylcyanurate	+	–	±	–	±	±	+	+
25	TTT	+	–	–	–	–	±	+	+
26	Divinylbenzene	–	–	–	–	–	–	±	±
27	TTT + NDMA (1 : 1)	++	+	++	+	++	++	++	++
28	TTT + NVP (1 : 1)	++	+	++	+	++	++	++	++
29	TTT + NDAPMA (2 : 1)	+	–	+	–	+	+	+	+
30	DMF–methanol (1 : 20)	++	–	–	–	–	±	+	+
31	DMF–methanol (1 : 4)	++	–	–	–	–	–	++	+
32	DMF–methanol (1 : 3)	++	–	±	–	–	–	++	+
33	DMF–methanol (1 : 1)	++	±	++	±	+	++	++	++
34	DMF–methanol (7 : 1)	++	++	++	++	++	++	++	++
35	DMF–acetonitrile (1 : 20)	++	-	-	-	-	+	+	+
36	DMF–toluene (1 : 20)	++	-	±	-	±	+	+	+
37	DMF–ether (1 : 20)	++	-	-	-	-	-	+	+
38	DMF–chloroform (1 : 20)	++	±	++	±	++	++	++	++

[a]Test: 10 mg/mL; ++, soluble; ±, partially soluble when heated; +, soluble when heated; –, insoluble. DMAc, dimethylacetamide; NMP, *N*-methylpyrrolidone; PY, pyridine; TTT, triallyltriazinetrione; NDMA, *N*-dimethylacrylamide; NVP, *N*-vinyl-2 pyrrolidone; NDAPMA, (*N*[(3-dimethylamino)propyl]methacrylamide).

$$\delta_v = 21.1 \mathrm{J}^{1/2}\mathrm{cm}^{3/2}$$

Hence, $\delta = 23.26\ \mathrm{J}^{1/2}/\mathrm{cm}^{3/2}$ thus (approximation) $\delta = 23.3\ \mathrm{J}^{1/2}/\mathrm{cm}^{3/2}$

These experimental solubility parameters are not separable, but they may be specified by the semi-empirical calculation (results summarized in Table V). The values of the solubility parameters calculated range between 22.4 and 23 $\mathrm{J}^{1/2}/\mathrm{cm}^{3/2}$ (Table V). Given the theoretical approximations and experimental uncertainty, these values are close to the value obtained graphically (23.3 $\mathrm{J}^{1/2}/\mathrm{cm}^{3/2}$). The values of the solubility parameters are high. They can be explained by the polarity of these BMIs. Indeed, these molecules contain polar groups (amide and ester),

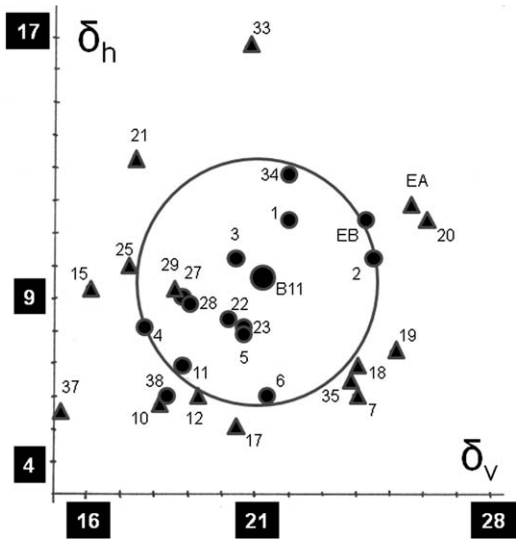

Figure 9. Ring solubility of B11 (example). EA: acetonitrile–water (80 : 20). EB: THF–EA (13 : 87). Solvent: ○; no solvent: Δ; No.: Table IV.

strongly polarizable groups (aramid and arylate types), and groups that could form hydrogen bonds (amide). All these polar groups increase the molecular interactions and cohesive energies (Ec).[99] As a result, there will be an increase in solubility parameter values (as $\delta = [Ec/V]^{1/2}$, V [molar volume]). The results summarized in Table V also show that these parameters of solubility decrease with the increase in the length of the BMI. This decrease may be explained by the apolar character of the group (—CH_2—) which allows the length of the molecule to increase. By increasing the length of the flexible grouping, the molecule becomes less polar and its parameter of solubility decreases.

On the basis of the results of the study of solubilities, a specific eluent to work in an isocratic system was developed. This optimization was conducted in three stages. A first eluent often used in HPLC was tested (EA). The eluent EA, consisting of an acetonitrile–water mixture (80/20), did not solubilize the BMI. This result was foreseeable from the graph of Figure 9. Indeed, the point of this mixture is out of the "circle of solubility." A new eluent with 87% of EA and 13% of THF was studied (EB). The addition of THF made it possible to obtain a point within the "circle of solubility" of BMI (EB point in Figure 9), but although this mixture (EB) solubilizes odd BMI very well it does not solubilize even BMI sufficiently (partial solubility). An interesting formulation for the four BMIs was obtained by adding a small amount of DMF just sufficient to thoroughly solubilize the even BMI (EC). The EC eluent contains 97% of EB and 3% of DMF.

The work on these solubilities of the BMI helped explain the effectiveness of the DMF–methanol (1/4) mixture schematically. Indeed, the first mixture DMF–methanol (1/4) is located outside the "circle of solubility" of these BMI ($\delta_h = 20.1$; $\delta_v = 20.07$). Then, in the "circle of solubility," the methanol ($\delta_h = 22.3$; $\delta_v = 19.55$) and DMF are not diametrically opposed,[15] as are, for example, the DMF and acetonitrile or DMF and chloroform (Figure 9). A small amount of methanol added to DMF moves it outside of the "circle of solubility." The purification test with the DMF–methanol (1/4) was carried out with B11. We achieved an excellent result. Impurities were removed without any BMI dissolution.[15] On the graph with all the compounds tested,[15] DMF–methanol (1/4) mixture is positioned correctly. Indeed, DMF–methanol (1/4) is sufficiently distant from the "circle of solubility" not partially to dissolve the BMI. In addition, it is not too far from the "circle of solubility" to remove impurities effectively enough (including impurities with molecular structures similar to the BMI: as a monomaleimide compound). Also, all BMIs synthesized were purified by precipitation with DMF–methanol (1/4).

Melting and Crosslinking Temperatures

After purification, the four BMIs were studied by DSC. The general appearance of the thermograms of these four BMIs, already published, is comparable (Figure 10). Endotherms and exotherms are easily observable. They show two effects of parity: crosslinking temperatures and melting points. Under the effect of heat, even BMIs and odd BMIs exhibit very different behaviors. Indeed, even BMI melting points are significantly higher than the odd BMI melting points (Table VI). Even BMIs crosslink quickly during fusion, whereas odd BMIs show distinctive endotherms and exotherms. Odd BMI showed definite distinction between the phenomena of fusion and the crosslinking. With even BMI, a rise in temperature (DSC: 20°C/min) makes it possible to improve the separation of the phenomena of fusion and crosslinking. In these circumstances, the exotherms are raised to higher temperatures. The fusion phenomenon becomes more complete. It can also be ascertained that enthalpies of fusion of even BMIs are higher than the enthalpies of fusion of odd BMIs (Table VI). The second effect of parity: crosslinking temperatures of even BMIs (exothermic peak) are lower than crosslinking temperatures of odd BMI. Even BMIs are thermally more reactive.

Table V. BMI-Solubility Parameters of Hansen (δ_x) Calculated from Hoftyzer–Van Krevelen[a] method[99]BMI

	V (cm^3/mol)	δ_d ($J^{1/2}/cm^{3/2}$)	δ_p ($J^{1/2}/cm^{3/2}$)	δ_h ($J^{1/2}/cm^{3/2}$)	δ_v ($J^{1/2}/cm^{3/2}$)	δ ($J^{1/2}/cm^{3/2}$)
B8	532.4	20.51	5.27	8.90	21.18	22.97
B9	548.9	20.39	5.11	8.77	21.02	22.78
B10	565.4	20.27	4.96	8.64	20.87	22.59
B11	581.9	20.16	4.82	8.51	20.73	22.41

[a]Molar volumes (V) calculated by Coleman method[101].

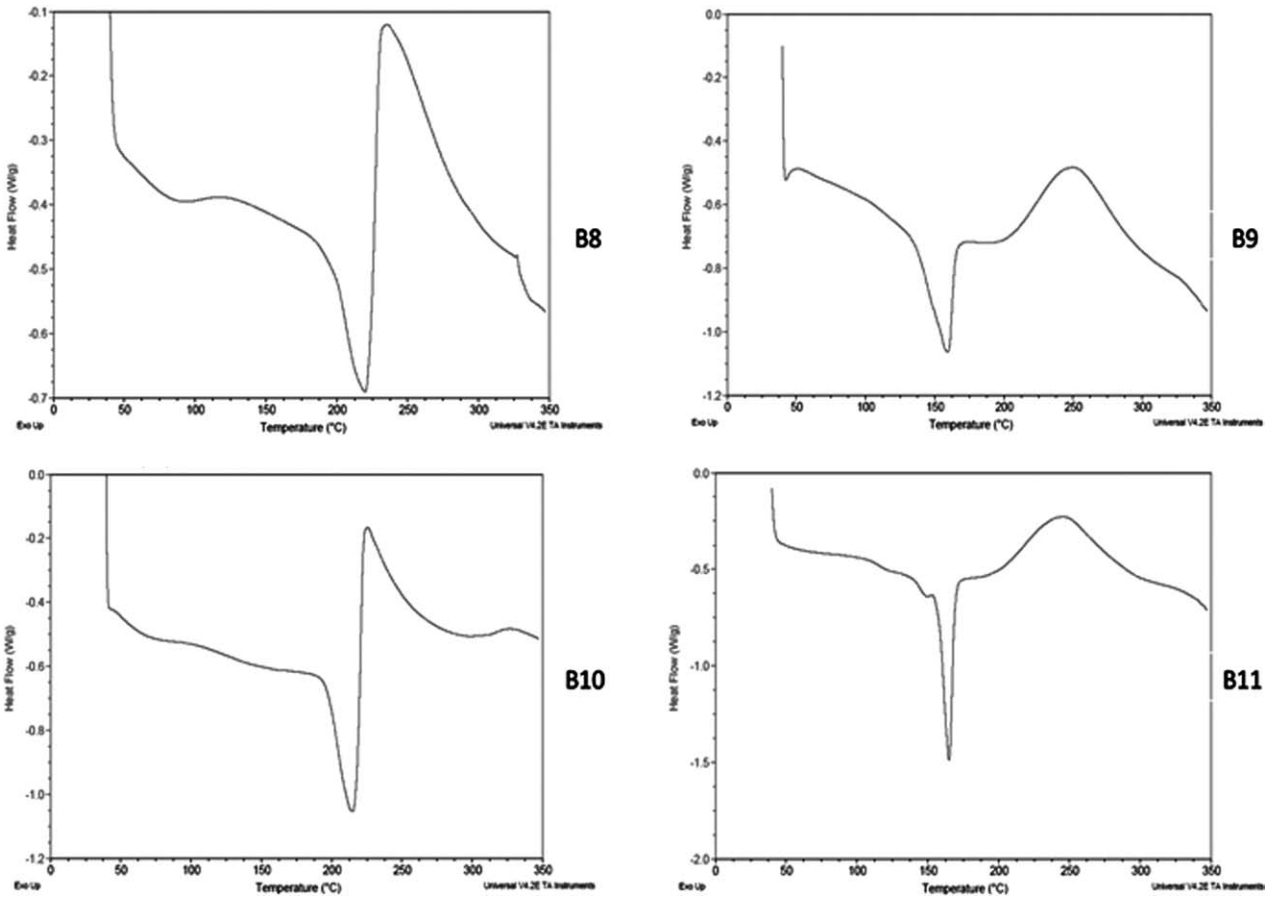

Figure 10. DSC thermograms of the synthesized BMI (B8, B9, B10, and B11) with 10°C/min.

Thermal Degradation

Crosslinking temperatures and melting points were determined by DSC. Work by TGA has enabled the heat resistance of each BMI to be determined. Our study shows that these BMIs, after crosslinking, show no degradation up to 350°C (Table VII: loss of 5% between 368 and 387°C). Depending on the BMI, the first significant degradation is located between 408 and 411°C. These results are interesting for polymers with polymethylenic flexible groupings. These results are also consistent with the results already obtained in the laboratory on the BMI LC "Arylates."[14] Indeed, with this type of BMI, the polymethylenic flexible grouping is the weak point for their thermal degradation. The BMI with many highly rigid aromatic nuclei have higher temperatures of degradation, often above 430°C. The amorphous BMIs with a flexible group show lower degradation temperatures located between 300 and 325°C.[11,102]

Two examples of thermogram are shown in Figure 11. Degradations occur more easily in the air (T_{d1} values: Table VII) but

Table VI. Melting Points and Crosslinking Temperatures of Pure BMI by DSC with 10 and 20°C/min[a]

BMI		T_f (°C)	ΔH_f (J/g)	T_r (°C)	ΔH_r (J/g)	Comments
B8	10°C/min	219.1[b]	41.08	233.1	73.52	Endotherm and exotherm poorly separated
	20°C/min	223.8[b]	63.83	251.0	83.25	
B9	10°C/min	159.2	40.69	251.3	106.3	Endotherm and exotherm separated
	20°C/min	162.3	42.01	266.2	108.7	
B10	10°C/min	210.9[b]	32.04	228.0	78.75	Endotherm and exotherm poorly separated
	20°C/min	220.0[b]	69.57	239.9	104.1	
B11	10°C/min	165.2	53.40	245.5	124.0	Endotherm and exotherm separated
	20°C/min	165.1	50.18	249.9	142.5	

[a]Crosslinking temperatures (T_r) and melting points (T_f) taken with the peaks of endotherms and exotherms. The enthalpies of melting and crosslinking are expressed in Joule per gram, [b]Endotherms broad.

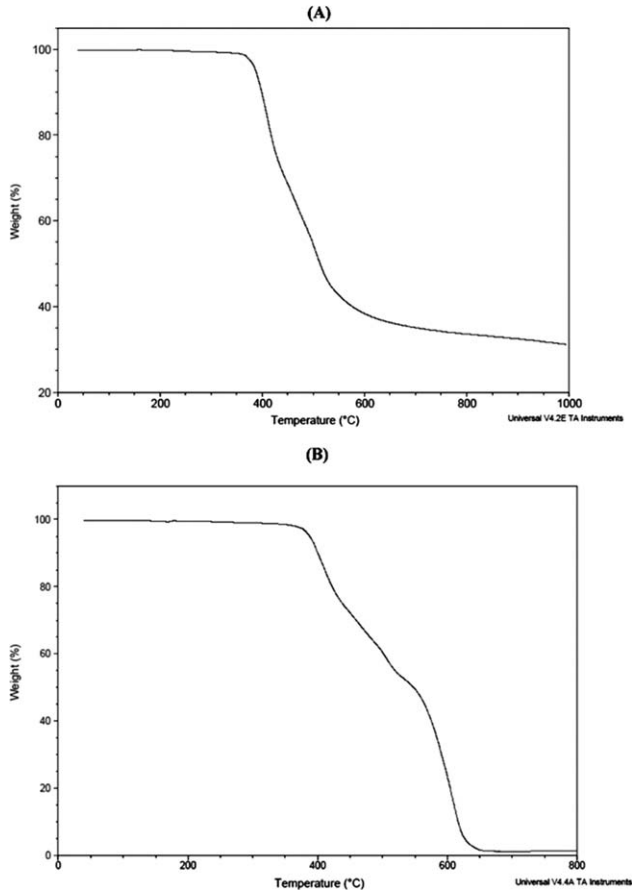

Figure 11. TGA thermograms of B11 with 10°C/min (crosslinked 1 h with 250°C): (A) under inert gas (nitrogen); (B) in the presence of air.

the differences, <8°C, are relatively low. On the other hand, for residues the differences are significant. Degradation in air is almost complete, whereas, under inert gas, the four BMI samples produce residues of between 30.36 and 35.02%. Thermograms obtained after crosslinking for 1 h at 250°C (exothermic peaks are located between 228 and 251°C) show that thermal degradations of these compounds take place at first approximation, from two kinetics. The first takes place at approximately at 410°C and the second at about 510°C.

The two results obtained (high degradation temperatures and small differences, 8°C, between under air and under inert gas) with the BMI (B8, B9, B10, and B11) may be explained by the presence of a liquid crystal state. Indeed, with the CLT the resistance to thermal oxidation is improved. There are two possible reasons for this phenomenon. These two reasons are based on the same findings: in the liquid crystal networks molecules are closer (LCD states are denser than amorphous states). The First reason: when the homolytic breakdown occurred, the two radicals obtained prior to complete separation, pass through an intermediate state called: "cage effect." Distances between molecules are small; these radical carbons can snatch radical hydrogens from neighboring molecules and become stable. The second reason: because for thermal oxidation to progress, become irreversible and catastrophic, it is necessary that formed radical carbons can fix oxygen. This oxygen, present outside the network, will have to diffuse through material. In this ordered material, which is much denser than the same material in its amorphous state, this diffusion will be more difficult. The resistance to thermal oxidation could thus be improved. As these original BMIs do not crosslink in the amorphous state, this assumption could not be checked within the framework of this study. Crosslinking which occurs during heating systematically produces an ordered liquid crystal state. However, the relatively high resistance to thermal oxidation of these materials as well as the slight variation observed between the tests carried out under air and under nitrogen could be explained partly by this mechanism.

Liquid Crystal Behavior

Thermal properties of B8, B9, B10, and B11 obtained from DSC can be correlated with properties determined by PLM. These BMIs show when heated two types of behavior. Odd BMI (B9 and B11) melt at relatively low temperatures (about 160°C) giving an amorphous state, whereas even BMI (B8 and B10) melt at very high temperatures (about 220°C), resulting in a liquid crystal state immediately after fusion. The thermal behavior of even BMI and odd BMI is different at the time of melting but

Table VII. BMI (After Crosslinking 1 h at 250°C)—Thermal Behavior Determined by TGA Under Air and Under Nitrogen[a]

	Under air				Under nitrogen		
BMI	$T_{5\%}$ (°C)	T_{d1} (°C)/ mass loss (%)	T_{d2} (°C)/ mass loss (%)	T_{d3} (°C)/ mass loss (%)	$T_{5\%}$ (°C)	T_{d1} (°C)/ mass loss (%)	T_{d2} (°C)/ mass loss (%)
B8	383	405	509	616	373	408	497
		23.17	20.78	54.97		32.82	32.71
B9	368	411	500	627	376	411	497
		26.06	21.59	50.60		46.90	26.38
B10	384	401	509	609	384	408	501
		25.40	15.12	56.22		27.56	36.96
B11	387	405	505	608	387	409	501
		26.82	20.14	51.40		40.25	27.01

[a] $T_{5\%}$ (T_d = 5% loss of mass).

Figure 12. B9-PLM (200×): After 1 h at 250°C, the compound shows a strong reflection of polarized light. [Color figure can be viewed in the online issue, which is available at wileyonlinelibrary.com.]

these two types of BMI, after complete crosslinking, lead to the formation of an ordered liquid crystal state of smectic type.

Odd BMIs (B9 and B11) have low melting points and pronounced fusion phenomena. Enthalpies of fusion of odd BMI (at 20°C/min) are much lower than the enthalpies of fusion of even BMI (Table VI). This result obtained by DSC was confirmed by the PLM study. Indeed, the PLM study shows close areas between the beginning of the transformation of the crystalline powder and the end of this transformation that provides a completely amorphous state.[15] Then, above the melting point, heating will produce an ordered crosslinked state characterized by reflection of polarized light (Figure 12). From 250°C in the area of presence of exotherm, polarized light reflection increases steadily. It may stabilize after complete crosslinking. With odd BMI crosslinking of the amorphous state provides an ordered state.[15]

The two even BMIs (B8 and B10) have similar high melting points (approximately, 220°C), determined by DSC. At 10°C/min, melting and crosslinking occur simultaneously. There is no clear separation between endotherm and exotherm (Figure 10). The PLM study confirmed this DSC result. Indeed, the PLM study at 10°C/min of B8 and B10 shows a difficult fusion. This fusion leads to a heterogeneous structure composed of colored

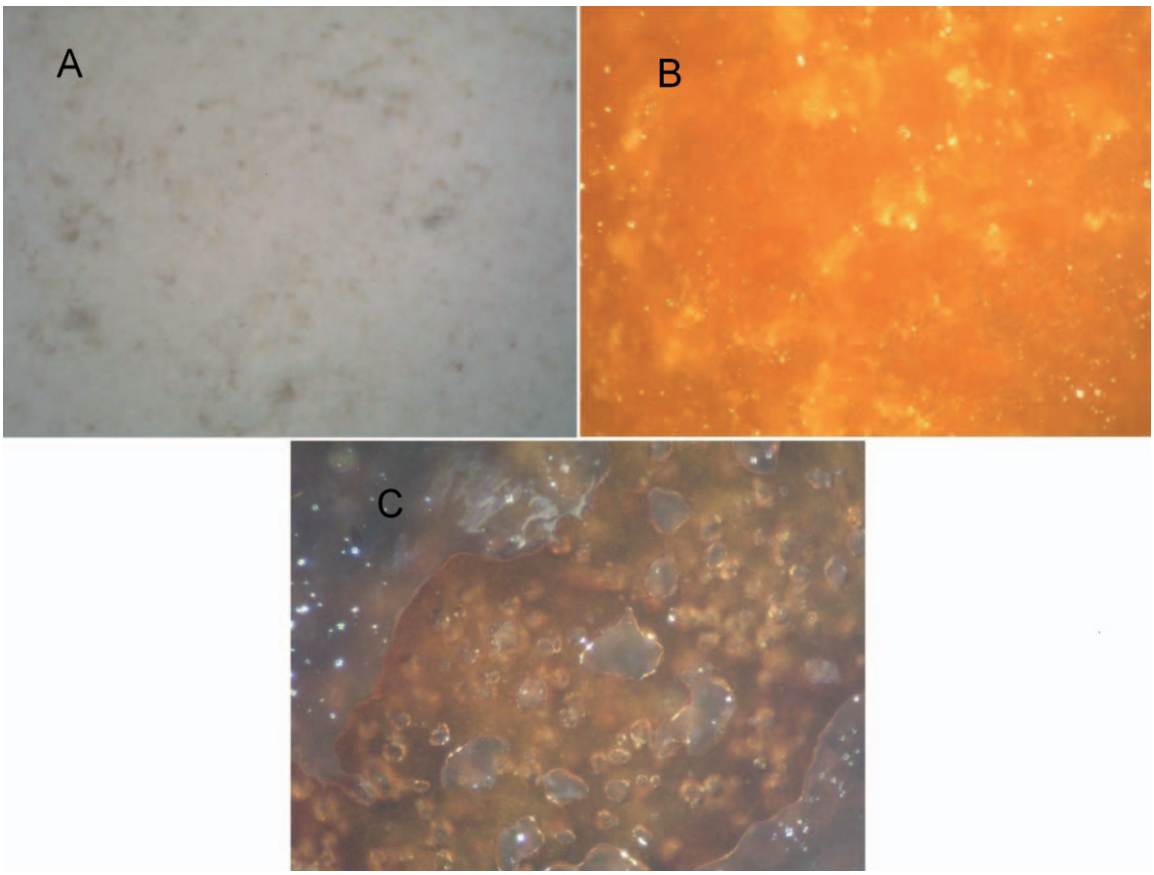

Figure 13. Melting of B8 with 20°C/min (PLM: 200×). (A) Crystalline powder ($T = 30$°C); (B) melting reveals a film colored ($T = 206$°C); (C) transformation toward the amorphous one ($T = 220$°C). [Color figure can be viewed in the online issue, which is available at wileyonlinelibrary.com.]

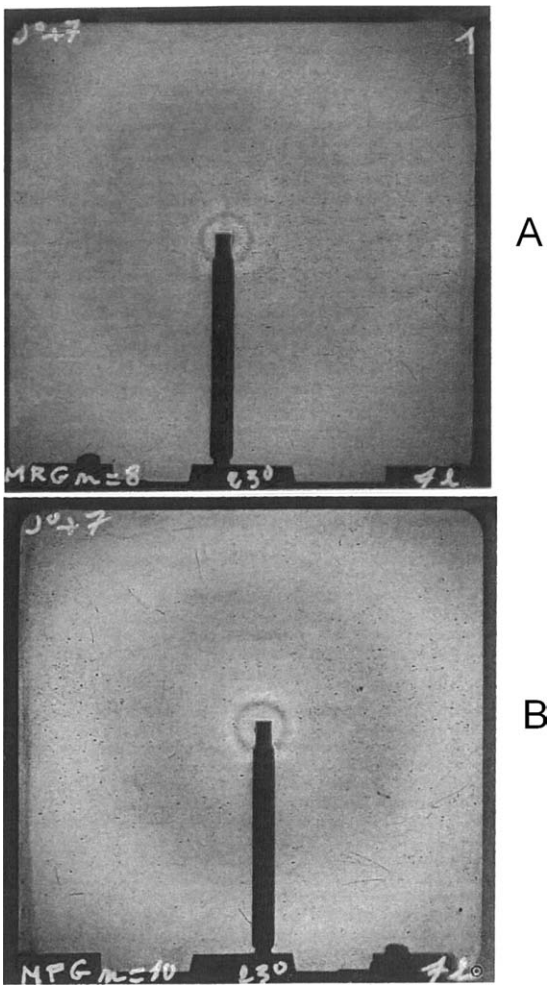

Figure 14. Pinhole camera powder X-ray diagrams of B8 (A) and B10 (B): realized after a crosslinking of 1 h with 250°C.

areas and black areas. When the heating is continued, black areas become colored areas.[15] At a much faster heating speed (20°C/min), B8 powder (or B10) melts more easily. Upon melting, the powder gives a film showing a uniform reflection of polarized light (Figure 13). Coloration appears at 201°C.[15] Beyond 201°C the coloring of the material intensifies. It is relatively constant between 206 and 209°C (Figure 13). Then beyond 209°C, the light reflection intensity decreases. An amorphous character appears. Finally, at higher temperatures (250°C), as in the test at 10°C/min, the amorphous character decreases. The solid again reflects light intensely.[15] The two types of tests with different heating rates show that fusion leads to an ordered state. The presence of this ordered state observed by PLM can be linked to the broad DSC endotherms (Table VI). With a low rise in temperature (10°C/min), these compounds crosslink quickly during their melting (transition: crystalline state/liquid crystal state). This will not result in a completely amorphous state. Crosslinking is promoted through the use of high temperatures, and also by the presence of a liquid crystal state. The material changes, during heating, to an entirely ordered state. Indeed, the amorphous areas are transformed into an ordered state by crosslinking, at high temperatures. At the end of the process, an ordered crosslinked network is obtained. With a very much higher increase in temperature (20°C/min), the transition crystalline state to liquid crystal state is less disrupted because crosslinking temperature is raised to higher temperatures (Table VI: approximately, 230–250°C). But the end of the process is the same because this BMI in the amorphous state will lead to an ordered state when heated. The four BMIs (B8, B9, B10, and B11) at the end of crosslinking give rise to an ordered state. With these BMIs, the ordered state obtained is liquid crystal type.

This liquid crystal state was characterized by PLM and X-R. It was initially characterized by PLM by the observation of a strong reflection of polarized light after melting and crosslinking of BMI.[15] Second, the presence of the liquid crystal state obtained after melting and crosslinking was confirmed by diffraction of X-rays (Figure 14). Small-angle X-ray scattering for crosslinked B8 corresponding to a smectic periodicity ($d = 35 \pm 1$ Å) (Figure 14). Comparison of d, the interlamellar distance, with the length of the repeating unit calculated from CHEM 3D software gives an angle of Tilt $\theta = 35°$ ($\cos \theta = d/l$). The spectrum of crosslinked B10 in the same conditions as B8 presents a periodicity of $d = 36 \pm 1$ Å and angle of Tilt $\theta = 37°$ (Figure 14). At large angles, for the two BMI, a more blurred stripe is observed at a distance of 5.7 Å. In our models, this value corresponds to the interchain distance.

X-ray spectra confirm the presence of a liquid crystal state. The study of these spectra helped to clarify the nature of smectic C liquid crystal state. This formation of a crosslinked liquid crystal state has already been characterized with "arylates" BMI of comparable structure having the same ester junctions and the same polymethylene flexible grouping at the center of the molecule.[14] During the course of the study, the smectic C liquid crystal structure was also characterized by X-R.[14]

The mechanisms of formation of a crosslinked network-ordered liquid crystal from an amorphous state are not very well known. Several hypotheses exist.[63,82,83,103] They can be used[82,83] for B8, B9, B10, and B11. In an isotropic state, the distribution of these molecules is statistical. Thermal agitation increased with heating. It will promote the statistical distribution of molecules. At a sufficiently high temperature, the BMI will react owing to their maleimide groups to give oligomers (dimers, trimers, etc.). These rigid, linear oligomers, could produce linear rod-shaped macromolecules. When the length of these rods is sufficient, a liquid crystal state may form. Indeed, according to the theory, high axial ratio (length/diameter) promotes the mesophase stability. Molecular interactions will become significant. Thermal agitation will not result in disorder. The oligomers will become ordered. They form a mesophase of smectic type. The amorphous state will turn into a mesomorphic state during crosslinking. Finally, crosslinking of ordered oligomers will give rise to a liquid crystalline network.

B8, B9, B10, and B11 reveal the effect of parity on solubilities, melting points, crosslinking temperatures (thermal reactivity) and the presence of a liquid crystal state upon melting. These effects of parity could be explained by differences in

conformation between even BMI and odd BMI. Indeed, even BMI possess greater linearity. MALEIMIDE-ARAMID-ARYLATE groups are rod shaped (calamitics). They constitute mesogen groups (linear, rigid, and strongly polarizable). Conformations possible between these rigid groups and the flexible group may explain the effect of parity. Indeed, with trans zig-zag conformation,[103] when the polymethylene flexible group has an even number of carbon atoms, it gives rise to a linear structure.[14,104–106] Odd BMIs give rise to nonlinear structures. More specifically with even BMI, there would be a greater number of conformations that would preserve the parallelism of mesogen groups contrary to the odd BMI.[107] Thus, even BMI molecules could be closer. These networks may be denser. This greater proximity could enable them to develop many more interactions. In addition, even BMI should reveal cohesive energies above those of odd BMI. Notice that these conformation questions are not taken into account by the methods of additivity of groups. These stronger interactions created by even BMI could explain their difficult solubilities and their particularly high melting points. Moreover, upon fusion, the more linear BMI will more easily promote the formation of a liquid crystal state.

Other authors have demonstrated that epoxide liquid crystals having a flexible polymethylene grouping at the center of the molecule and ester junctions gave rise to the smectic C mesophase.[73,74] The ester group could promote the smectic character by a further polarization and an increase in the length of the mesogen group (conjugation). The long flexible group located in the center of the molecule promotes the smectic mesophase by an increase in flexibility. This additional flexibility enables the rigidity brought about by crosslinking to be overcome. But in the case of the flexible groups being too long the liquid crystal character could disappear. A flexible grouping, which is too long, may lead to the molecule being too flexible. This could be problematic for the liquid crystal state.[75]

CONCLUSION

The syntheses of these BMIs were carried out under good conditions with excellent yields. The study of the solubilities of these BMI enabled these BMIs to be purified from solvent (DMF) and a nonsolvent (methanol). The effectiveness of the purification method was tested by HPLC. Purity rates exceeded 94%. The solubility parameters of these BMI, determined experimentally, and estimated by a semi-empirical calculation method, are relatively high (about 23 $J^{1/2}/cm^{3/2}$). These pure BMIs have degradation temperatures of the order of 410°C. Differences between temperatures of degradation in air or in an inert atmosphere are low (approximately, 8°C). These BMIs show four effects of parity: solubilities, melting points, crosslinking temperature, and the appearance of a liquid crystal state on melting. Indeed, even BMIs are more difficult to dissolve, their melting points are much higher, their crosslinking temperatures are lower and they give rise to an ordered state upon melting. These effects of parity can be explained schematically by the more linear conformations of even BMI. But the odd BMIs, like the even BMI, give rise to an ordered liquid crystal state after crosslinking. This smectic liquid crystal state (type C) was characterized by PLM and X-R.

ACKNOWLEDGMENTS

This work received the support of the Agence Universitaire de la Francophonie (AUF).

REFERENCES

1. Tang, H.; Song, N.; Chen, X.; Fan, X.; Zhou, Q. *J. Appl. Polym. Sci.* **2008,** *109*, 190.
2. Zhang, X.; Jin, Y.; Diao, H.; Du, F.; Li, Z.; Li, F. *Macromolecules* **2003,** *36*, 3115.
3. Varma, I. K.; Fohlen, G. M.; Parker, J. A. *J. Polym. Sci.: Polym. Chem. Ed.* **1982,** *20*, 283.
4. Amutha, N.; Sarojadevi, M. *J. Appl. Polym. Sci.* **2008,** *110*, 1905.
5. Tang, H.; Song, N.; Gao, Z.; Chen, X.; Fan, X.; Xiang, Q.; Zhou, Q. *Polymer* **2007,** *48*, 129.
6. Tang, H.; Song, N.; Gao, Z.; Chen, X.; Fan, X.; Xiang, Q.; Zhou, Q. *Eur. Polym. J.* **2007,** *43*, 1313.
7. Sava, M. *J. Appl. Polym. Sci.* **2009,** *112*, 1399.
8. Sava, M.; Sava, I.; Cozan, V.; Tanasa, F. *J. Appl. Polym. Sci.* **2007,** *106*, 2185.
9. Sava, M.; Gaina, C.; Gaina, V.; Chiriac, C.; Stoleriu, A. *JMS Pure Appl. Chem.* **1997,** *34*, 1505.
10. Kumar, K. S. S.; Nair, C. P. R.; Sadhana, R.; Ninan, K. N. *Eur. Polym. J.* **2007,** *43*, 5084.
11. Sava, M. J. *Appl. Polym. Sci.* **2006,** *101*, 567.
12. Mikroyannidis, J. A.; Melissaris, A. P. *J. Appl. Polym. Sci.* **1989,** *37*, 2587.
13. Belina, K. *J Thermal Anal.* **1997,** *50*, 655.
14. Kallal-Bartolomeo, K.; Milano, J. C.; Vernet, J. L.; Gallot, B. *Macromol. Chem. Phys.* **2000,** *201*, 2276.
15. Pham, Q. T. R.Thesis December 2010, Université du Sud Toulon Var.
16. Milano, J. C.; Mekkid, S.; Vernet, J. L. *Eur. Polym. J.* **1997,** *33*, 1333.
17. Hao, J.; Wang, W.; Jiang, B.; Cai, X.; Jiang, L. *Polym. Int.* **1999,** *48*, 235.
18. Milano, J. C.; Mekkid, S.; Vernet, J. L. *Macromol. Chem. Phys.* **1996,** *197*, 3837.
19. Fache, B.; Mekkid, S.; Milano, J. C.; Vernet, J. L. *Eur. Polym. J.* **1998,** *34*, 1621.
20. Milano, J. C.; Mekkid, S.; Vernet, J. L. *Eur. Polym. J.* **1998,** *34*, 717.
21. Shau, M.; Tsai, P.; Teng, W.; Hsu, W. *Eur. Polym. J.* **2006,** *42*, 1899.
22. Hariharan, R.; Sarojadevi, M. J. *Appl. Polym. Sci.* **2008,** *108*, 1126.
23. Goldfarb, I. J.; Feld, W. A.; Saikumar, J. *Polymer* **1993,** *34*, 813.
24. Jeng, R.; Chang, C.; Chen, C. P.; Chen, C. T.; Su, W. *Polymer* **2003,** *44*, 143.
25. Hwang, H.; Li, C.; Wang, C. *Polymer* **2006,** *47*, 1291.

26. Seo, J.; Lee, C.; Jang, W.; Sundar, S.; Han, H. *J. Appl. Polym. Sci.* **2006,** *99*, 1692.
27. Rao, B. S.; Sireesha, R.; Pasala, A. R. *Polym. Int.* **2005,** *54*, 1103.
28. Pouzols, G.; Rakoutz, M. *SAMPE Symposium* **1985,** March 19–21, 606.
29. Rakoutz, M.; Balme, M. *Polym. J.* **1987,** *19*, 173.
30. Sava, M. J. *Appl. Polym. Sci.* **2002,** *84*, 750.
31. Kumar, R. S.; Alagar, M. *J. Appl. Polym. Sci.* **2006,** *101*, 668.
32. Musto, P.; Ragosta, G.; Russo, P.; Mascia, L. *Macromol. Chem. Phys.* **2001,** *202*, 3445.
33. Yan, H. Q.; Wang, H. Q.; *Cheng, J Eur. Polym. J.* **2009,** *45*, 2383.
34. Liu, X.; Yu, Y.; Li, S. *Polymer* **2006,** *47*, 3767.
35. Gu, A. *Compos. Sci. Technol.* **2006,** *66*, 1749.
36. Fan, J.; Hu, X.; Yue, C. Y. *J. Appl. Polym. Sci.* **2003,** *88*, 2000.
37. Chaplin, A.; Hamerton, I.; Herman, H.; Mudhar, A. K.; Shaw, S. J. *Polymer* **2000,** *41*, 3945.
38. Dao, B.; Hodgkin, J.; Krstina, J.; Mardel, J.; Tian, W. *J. Appl. Polym. Sci.* **2007,** *105*, 2062.
39. Luo, Z.; Liu, F.; Wei, L.; Zhao, T. *Polym. Comp.* **2007, 180.**
40. Nair, C. P. R. *Prog. Polym. Sci.* **2004,** *29*, 401.
41. Gouri, C.; Nair, C. P. R.; Ramaswamy, R. *Polym. Polym. Comp.* **2003,** *11*, 311.
42. Li, Y.; Morgan, R. J.; Tschen, F.; Sue, H.; Lopata, V. J. *Appl. Polym. Sci.* **2004,** *94*, 2407.
43. Shanmugam, V.; Chinnaswamy, T. V.; Sarfaraz, A.; Sankaran, N. *Eur. Polym. J.* **2009,** *45*, 1271.
44. Yan, H.; Ning, R.; Liang, G.; Ma, X. *J. Appl. Polym. Sci.* **2005,** *95*, 1246.
45. Jin, L.; Agag, T.; Ishida, H. *Eur. Polym. J.* **2010,** *46*, 354.
46. Chu, P. P.; Wu, C. S.; Liu, P. C.; Wang, T. H.; Pan, J. P. *Polymer* **2010,** *51*, 1386.
47. Hopewell, J. L.; George, G. A.; Hill, D. J. T. *Polymer* **2000,** *41*, 8231.
48. Hopewell, J. L.; George, G. A.; Hill, D. J. T. *Polymer* **2000,** *41*, 8221.
49. Mison, P.; Sillion, B. *Adv. Polym. Sci.* **1999,** *140*, 138.
50. Curliss, D. B.; Cowans, B. A.; Caruthers, J. M. *Macromolecules* **1998,** *31*, 6776.
51. Dix, L. R.; Ebdon, J. R.; Flint, N. J.; Hodge, P.; O'Dell, R. *Eur. Polym. J.* **1995,** *31*, 647.
52. Rozenberg, B. A.; Dzhavadyan, E. A.; Morgan, R.; Shin, E. *Macromol. Symp.* **2001,** *171*, 87.
53. Matsumoto, A. *Prog. Polym. Sci.* **2001,** *26*, 189.
54. Zhang, X.; Du, F.; Li, Z.; Li, F. *Macromol. Rapid Commun.* **2001,** *22*, 983.
55. Hopewell, J. L.; Hill, D. J. T.; Pomery, P. *J. Polymer* **1998,** *39*, 5601.
56. Grenier-Loustalot, M.; Da Cunha, L. *Polymer* **1997,** *39*, 1833.
57. Phelan, J. C.; Sung, C. *Macromolecules* **1997,** *30*, 6845.
58. Grenier-Loustalot, M.; Gouarderes, F.; Joubert, F.; Grenier, P. *Polymer* **1993,** *34*, 3848.
59. Zainol, I.; Day, R.; Heatley, F. *J. Appl. Polym. Sci.* **2003,** *90*, 2764.
60. Abadie, M. J. M.; Xiong, Y.; Boey, F. Y. C. *Eur. Polym. J.* **2003,** *39*, 1243.
61. Gu, A.; Liang, G.; Liang, D.; Ni, M. *Polym. Adv. Technol.* **2007, 835.**
62. Shiota, A.; Ober, C. *Prog. Polym. Sci.* **1997,** *22*, 975.
63. Barclay, G.; Ober, C. *Prog. Polym. Sci.* **1993,** *18*, 899.
64. Hikmet, R. A. M.; Broer, D. *J. Polymer* **1991,** *32*, 1627.
65. Hölter, D.; Fray, H.; Mülhaupt, R.; Klee, J. E. *Macromolecules* **1996,** *29*, 7003.
66. Shiota, A.; Ober, C. K. *J. Polym. Sci. Polym. Chem.* **1996,** *34*, 1291.
67. Barclay, G.; Ober, C.; Papathomas, K.; Wang, D. *J. Polym. Sci. A: Polym. Chem.* **1992,** *30*, 1831.
68. Jahromi, S.; Lub, J.; Mol, G. N. *Polymer* **1994,** *35*, 622.
69. Barclay, G.; MacNamee, S.; Ober, C.; Papathomas, K.; Wang, D. *J. Polym. Sci. A: Polym. Chem.* **1992,** *30*, 1845.
70. Galina, H.; Mossety-Lesczak, B. *J. Appl. Polym. Sci.* **2007,** *105*, 224.
71. Castell, P.; Serra, A.; Galià, M. *J. Polym. Sci. A: Polym. Chem.* **2004,** *42*, 3631.
72. Ortiz, C.; Kim, R.; Rodighiero E.; Ober, C. K.; Kramer, E. J. *Macromolecules* **1998,** *31*, 4074.
73. Ribera, D.; Mantecon, A.; Serra, A. *Macromol. Symp.* **2003,** *199*, 267.
74. Ribera, D.; Serra, A.; Mantecon, A. *J. Polym. Sci. A: Polym. Chem.* **2003,** *41*, 1465.
75. Ribera, D.; Mantecon, A.; Serra, A. *Macromol. Chem. Phys.* **2001,** *202*, 1658.
76. Carfagna, C.; Amendola, E.; Giamberini, M. *J. Mater. Sci. Lett.* **1994,** *13*, 126.
77. Mormann, W.; Kuckertz, C.; Bröcher, M. *Macromol. Symp.* **2010,** *290*, 70.
78. Wlodarska, M.; Bak, G.; Mossety-Leszczak, B.; Galina, H. *J. Mater. Process. Technol.* **2009,** *209*, 1662.
79. Lee, J.; Jang, J. *Polymer* **2006,** *47*, 3036.
80. Vyazovkin, S.; Mititelu, A.; Sbirrazzuoli, N. *Macromol. Rapid Commun.* **2003,** *24*, 1060.
81. Punchaipetch, P.; Ambrogi, V.; Giamberini, M.; Brostow, W.; Carfagna, C.; D'souza, N. *Polymer* **2002,** *43*, 839.
82. Hoyt, A.; Benicewicz, B. *J. Polym. Sci. Polym. Chem.* **1990,** *28*, 3403.
83. Hoyt, A.; Benicewicz, B. *J. Polym. Sci. Polym. Chem.* **1990,** *28*, 3417.
84. Hoyt, A.; Huang, S. *J. JMS Pure Appl. Chem.* **1995,** *A 32*, 1931.
85. Liu, X.; Mi, J.; Gu, Y.; Jiang, L.; Cai, X. *Gaofenzi Cailiao Kexue Yu Goncheng* **1995,** *11*, 112.

86. Liu, X.; Gu, Y.; Jiang, L.; Cai, X. *Gaofenzi Cailiao Kexue Yu Goncheng* **1995,** *11*, 46.
87. Liu, X.; Jiang, L.; Cai, X. *Hecheng Shuzhi Ji Suliao* **1997,** *14*, 19.
88. Mi, J.; Liu, X.; Zhang, X.; Li, Z.; Cai, X. *Hecheng Huaxue* **1997,** *5*, 377.
89. Mi, J.; Zhang, X.; Li, Z.; Liu, X.; Cai, X. *Reguxing Shuzhi* **1997,** *12*, 5.
90. Imai, M.; Frings, R.; Grahe, G.; Kawamura, J.; Obi, N. Patent EP 1 016 659 A1, **2000.**
91. Cozan, V.; Sava, M.; Marin, L.; Bruma, M. *High Perform. Polym.* **2003,** *15*, 301.
92. Ahn, Y.; Jung, M.; Chang, J. *Mater. Chem. Phys.* **2010,** *123*, 177.
93. Mikroyannidis, J. A. *J. Polym. Sci. A: Polym. Chem.* **1990,** *28*, 679.
94. Stenzenberger, H. D.; Herzog, M.; Römer, W.; Scheiblich, R.30th National SAMPE Symposium 1985, March, 19.
95. Hansen, C. J. *Paint Technol.* **1967,** *39*, 505, 104.
96. Hansen, C. J. *Paint Technol.* **1967,** *39*, 511, 505.
97. Hansen, C.; Skaarup, K. J. *Paint Technol.* **1967,** *39*, 511, 511.
98. Hansen, C. *I and EC Product Research and Development* **1969,** 8, March 2.
99. Van Krevelen, D. W. Properties of Polymers; Elsevier: Amsterdam-London-New York-Tokyo, **1990;** p 189.
100. Bellenger, V. *Composites* **1996,** *17*, 48.
101. Coleman, M. M.; Serman, C. J.; Bhagwagar, D. E.; Painter, P. C. *Polymer* **1990,** *31*, 1187.
102. Sava, M.; Gaina, C.; Gaina, V.; Timpu, D. *Macromol. Chem. Phys.* **2001,** *202*, 2601.
103. Shiota, A.; Ober, C. K. *Polymer* **1997,** *38*, 23, 5857.
104. Jin, J. *J. Mol. Cryst. Liq. Cryst.* **1995,** *267*, 249.
105. Griffin, A. C.; Vaidya, S. R.; Hung, R. S. L.; Gorman, S. *Mol. Cryst. Liq. Cryst. Lett.* **1985,** *1*, 131.
106. Jin, J.; Chung, Y.; Lenz, R. W.; Ober, C. *Bull. Korean Chem. Soc.* **1983,** *4*, 143.
107. Date, R. W.; Imrire, C. T.; Luckhurst, G. R.; Seddon, J. M. *Liq. Cryst.* **1992,** *12*, 203.